Simplified Steady State Analysis of Stand-Alone Doubly Fed Induction Generator

M. Sharawy
Electrical Engineering Department
Faculty of Engineering at Shoubra, Benha University
Cairo, Egypt
mohamed.anwer@feng.bu.edu.eg

Adel A. Shaltout
Electrical Power and Machines Department
Faculty of Engineering, Cairo University
Cairo, Egypt
aashaltout@yahoo.com

N. Abdel-Rahim
Electrical Engineering Department
Faculty of Engineering and Technology, Future University in Egypt
Cairo, Egypt
naser.abdelrahim@fue.edu.eg

O. E. M. Youssef
Electrical Engineering Department
Faculty of Engineering at Shoubra, Benha University
Cairo, Egypt
omar.youssef@feng.bu.edu.eg

Mahmoud A. Al-Ahmar
Electrical Engineering Department
Faculty of Engineering at Shoubra, Benha University
Cairo, Egypt
ma_alahmar2@hotmail.com

***Abstract* – This paper presents the steady state analysis and characteristics of a doubly-fed induction generator (DFIG) employed in stand-alone wind energy conversion system (WECSs) in a similar way as the synchronous generator. The DFIG is excited through the rotor terminals by a slip-frequency voltage and current injected to the rotor from a battery via rotor side converter. A simplified mathematical model required for evaluation of the steady state analysis and characteristics of the DFIG is presented. The effect of load variation on the rotor voltage, active and reactive power when the generator operated at constant speed is studied. Also, the effect of the generator speed variation when operated at constant load on the rotor voltage, active and reactive power is illustrated. The results show that the parameters affected on the steady state analysis and characteristics of the DFIG by using this method is more clearly and simply.**

Index Terms* – *Steady state analysis, Stand-alone WECS, DFIG, Mathematical model.

I. INTRODUCTION

In modern decades, the doubly fed induction generator (DFIG) is considered as a suitable electrical generator which can be used in stand-alone wind energy conversion system (WECS) as it can operate at variable speed with constant output voltage and frequency [1], [2]. Also, it has numerous advantages such as reduced power converter rating, operation under variable speed, less losses with improved efficiency, decoupled active and reactive power control, and economically wise [3], [4], [5].

DFIG can supply power to an isolated load at constant voltage and frequency irrespective of the variation of wind speed and the connected loads. The main configuration of a stand-alone WECS based on DFIG is shown in Fig. 1 [6]. In order to achieve constant voltage and frequency most of authors have suggested the field-oriented control (FOC) strategy [7], [8]. The output voltage is regulated indirectly by controlling the amplitude of the excitation current of the rotor (regulating the flux in the machine) while the output frequency is kept constant by imposing rotor currents with slip frequency [7], [8]. The usage of bi-directional AC-AC converter connected to the rotor circuit contributes to expand the range of operating speed above synchronous speed and enable power production from both the stator side and rotor side. This converter consists of rotor side converter (RSC) and load side converter (LSC). RSC is used to control the stator voltage and frequency and LSC is used to regulate the DC bus voltage, harmonics compensation and load balancing [6], [9]-[11].

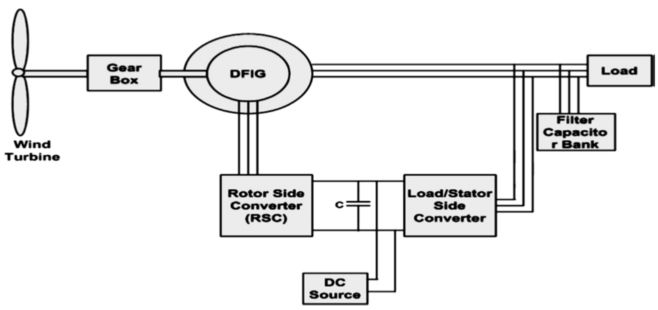

Fig. 1 Main configuration of stand-alone WECS based on DFIG.

When the DFIG supplies an isolated load at constant stator output voltage and frequency, the generator may operate at two modes of operation according to the generator speed: sub-synchronous and super-synchronous speed modes of operation [12]. The changing of operating speed, hence operating slip, requires continuous changing in rotor input voltage and frequency, consequentially the rotor active and reactive power to maintain the stator outputs constant. The variation of those parameters must be taken into consideration during the generator operation for optimum operation. This can be achieved by the correct study of the characteristics of the generator at different operating conditions.

The growing development of the wind energy for electrical power generation using DFIG will have a substantial influence on the stability of the power system [13]. Wherefore, DFIG must be modeled properly in power system

978-1-6654-1998-7/21/$31.00 ©2021 IEEE

stability analysis. Also, the analysis of the steady state performance of DFIG under different operating condition is required so that the required power can be generated properly at any point of operation specially when the DFIG operates at maximum power point condition [14]. Many authors in [12]-[20] have been evaluated the steady state analysis and characteristics of grid connected DFIG based on its conventional equivalent circuit under different operating conditions. However, the evaluation of the steady state analysis and characteristics of DFIG in stand-alone operation is presented only in [15]. But such those computations in both cases are quite difficult and require long time with fatigued mathematical procedures.

In this paper the steady state analysis and characteristics of the stand-alone DFIG are presented. The DFIG is assumed to be excited through the rotor terminals with a slip frequency voltages and currents comes from a battery and RSC. This cause the rotational speed of the resulting magnetic field in the air gap is always at synchronous speed and independent of the DFIG rotational speed. A simplified mathematical model required for evaluation of the steady-state analysis and characteristics of the DFIG is presented in a similar way as the synchronous generator. The effect of load variation on the rotor voltage, active and reactive power when the generator runs at constant speed is studied. Also, the effect of the generator speed variation on the rotor voltage, active and reactive power is illustrated.

II. Simplified Mathematical Model of DFIG

The conventional per phase equivalent circuit of a DFIG in steady state is shown in Fig. 2. The stator and rotor equations which represent the voltages and currents as functions of DFIG parameters are presented as follows [21], [22]:

$$\vec{E}_m = \vec{V}_s + \vec{I}_s(R_s + jX_{Ls}) \tag{1}$$,

$$\vec{E}_m = jX_m\vec{I}_m \tag{2}$$,

$$\vec{I}_m = -(\vec{I}_s + \vec{I}_r) \tag{3}$$,

$$\vec{V}_r / s = \vec{E}_m - \vec{I}_r(R_r / s + jX_{Lr}) \tag{4}$$,

Where,

$\vec{V}_s$ is the stator output voltage phasor with frequency f_s,
R_s is the stator winding resistance,
X_{Ls} is the stator winding leakage reactance,
X_m is the magnetizing reactance,
$\vec{I}_s$ is the stator current phasor,
$\vec{I}_m$ is the magnetizing current phasor,
X_{Lr} is the rotor winding leakage reactance referred to stator,
R_r is the rotor winding resistance referred to stator,
$\vec{V}_r$ is the supplied rotor voltage phasor referred to stator,
$\vec{I}_r$ is the rotor current phasor referred to stator,
$\vec{E}_m$ is the mutual induced voltage phasor, and
s is the slip and is given by:

$$s = \frac{N_s - N}{N_s} \tag{5}$$,

where

N_s is the synchronous speed of the DFIG at certain stator output frequency, and
N is speed of the rotor shaft of the DFIG.

Substituting (3) into (2) then:

$$\vec{E}_m = \vec{E}_{os} - jX_m\vec{I}_s \tag{6}$$,

$$\vec{E}_{os} = -jX_m\vec{I}_r \tag{7}$$.

Substituting (6) into (1) gives

$$\vec{E}_{os} = \vec{V}_s + \vec{I}_s(R_s + jX_s) \tag{8}$$.

Substituting (2) and (3) in (4) gives

$$\begin{aligned}\vec{V}_r = \vec{I}_r[(-R_r - sX_m\frac{I_s}{I_r}\sin(\theta_{Is} - \theta_{I_r})) + \\ j(-sX_r + sX_m\frac{I_s}{I_r}\cos(\theta_{Is} - \theta_{I_r}))]\end{aligned} \tag{9}$$.

Where

X_s the total stator winding reactance (X_m+X_{Ls}),
X_r is the total rotor winding reactance (X_m+X_{Lr}),
$\vec{E}_{os}$ is the generator e.m.f at no-load,
δ is the angle between $\vec{E}_{os}$ and $\vec{V}_s$, power angle,

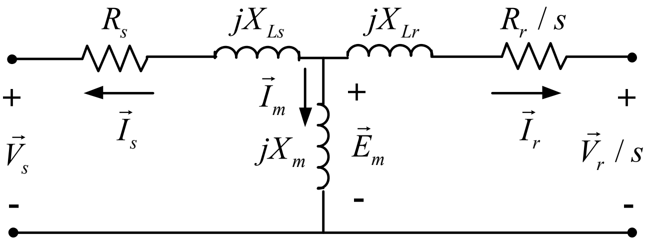

Fig. 2 DFIG equivalent circuit per phase in steady state.

θ_{Is} is the angle between $\vec{I}_s$ and $\vec{V}_s$,power factor angle, and
θ_{Ir} is the angle between $\vec{I}_r$ and $\vec{V}_s$.

Assume the stator current lags the stator voltage by an angle φ, (9) can be simplified as

$$\begin{aligned}\vec{V}_r = -\vec{I}_r[(R_r + sX_m\frac{I_s}{I_r}\cos(\varphi + \delta)) + \\ j(sX_r - sX_m\frac{I_s}{I_r}\sin(\varphi + \delta))] = -\vec{I}_r(R_{rt} + jX_{rt})\end{aligned} \tag{10}$$,

$$V_r = I_r\sqrt{R_{rt}^2 + X_{rt}^2} \tag{11}$$,

where,

R_{rt} is the rotor total equivalent resistance,
X_{rt} is the rotor total equivalent reactance,
I_s is the rms of the stator current,
I_r is the rms of the rotor current, and
V_r is the rms of the rotor voltage.

As indicated by (10), R_{rt} and X_{rt} are functions of stator and rotor currents, power angle, slip, and stator output frequency. The simplified equivalent circuit can be deduced from (8) and (10) shown in Fig. 3.

III. Steady State Analysis of DFIG

From the simplified equivalent circuit in Fig. 3, the stator equivalent circuit representation is similar to the stator of the synchronous generator equivalent circuit. Also, neglecting the stator winding resistance, the voltage phasor diagram of the stator equivalent circuit with lagging power factor is illustrated in Fig. 4.a [21].

From the voltage phasor diagram, the corresponding power units diagram can be obtained by changing the scale of its axes from volts to voltamperes using the conversion factor $3V_s / X_s$ as shown in Fig. 4.b [23].

From the phasor diagram, and eq. (7) the stator apparent, active, and reactive power can be obtained as follows [21], [22]:

$$S_s = 3\vec{V}_s \vec{I}_s^* = P_s + jQ_s \quad (12),$$

$$P_s = \frac{3V_s I_r X_m}{X_s} \sin\delta \quad (13),$$

$$Q_s = \frac{3V_s I_r X_m}{X_s} \cos\delta - \frac{3V_s^2}{X_s} \quad (14),$$

Neglecting the rotor resistive losses, the rotor apparent, active, and reactive power can be expressed as follows [21], [22]:

$$S_r = 3\vec{V}_r \vec{I}_r^* = P_r + jQ_r \quad (15)$$

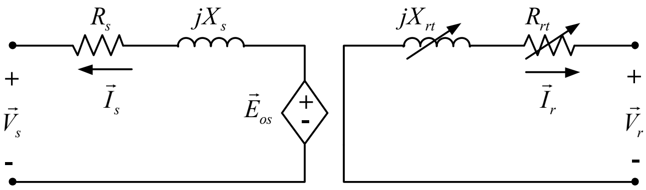

Fig. 3 Simplified equivalent circuit of DFIG.

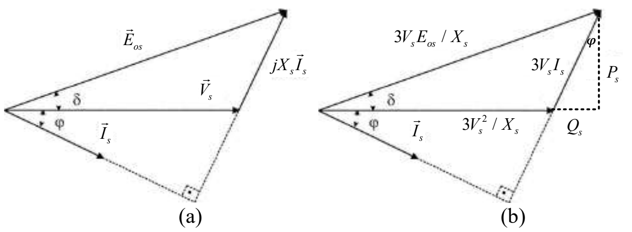

Fig. 4. (a) DFIG Stator phasor diagram (b) Corresponding power units diagram.

$$P_r = -s\frac{3V_s I_r X_m}{X_s} \sin\delta \quad (16)$$

$$Q_r = -s[3I_r^2 X_r + \frac{3V_s I_r X_m}{X_s} \cos\delta - \frac{3I_r^2 X_m^2}{X_s}] \quad (17)$$

IV. Steady State Characteristics of DFIG

For evaluation the steady state characteristics of the DFIG, the stator of the DFIG is assumed to be connected to stand-alone load at constant voltage and frequency. Also, the DFIG is assumed to be excited through the rotor terminals with a slip frequency voltages and currents comes from a battery and RSC. This cause the rotational speed of the resulting magnetic field in the air gap is always at synchronous speed and independent of the DFIG rotational speed. A 15 kW DFIG with parameters depicted in Table.1 [24] is used to evaluate the steady state characteristics.

A. Effect of load variation on the DFIG operated at constant speed

In this study, the DFIG is assumed to be operated at constant two different operating speeds, first on is 1350 rpm (s = 0.1) for sub-synchronous speed mode of operation. The second one is 1650 rpm (s = - 0.1) for super-synchronous speed mode of operation.

For both operating speeds, the power angle δ is varied from 0° to 180°. All results are given in per-unit with base voltage of 220 V, base current of 32 A and base apparent power of 21120 VA.

Table.1: DFIG parameters

Parameter	Value	Parameter	Value
Rated power	15 kW	Number of poles	4
Operating frequency	50 Hz	Turns ratio	1
Synchronous speed	1500 rpm	R_s	161 mΩ
Rated stator line voltage	380 V (rms)	L_{Ls}	3 mH
Rated stator current	32 A	L_m	46.5 mH
Rated rotor current	46 A	R_r	178 mΩ
Stator connection	Star	L_{Lr}	3 mH

Fig. 5 shows the stator output active power, P_s, versus power angle δ at rotor current I_r = 1 and 0.5 p.u. As shown, the P_s varies sinusoidally with δ. At certain I_r, 0.5 p.u, the DFIG can be loaded gradually until the limit of P_{max1} where the δ reaches to its static stability limits of 90°. For δ larger than 90°, the DFIG will operate at unstable operating region. At certain power angle, δ_o, and rotor current equal 0.5 p.u, the DFIG stator output power capability can be increased from P_{L1} to P_{L2} by increasing the rotor current to 1 p.u.

Fig. 6 shows the stator output reactive power, Q_s, versus power angle δ at rotor current I_r = 1 and 0.5 p.u. Unlike P_s versus δ curve, as the δ increases the Q_s decreases. The maximum Q_s can be obtained at δ = 0°. Also, the DFIG stator output reactive power capability can be increased from Q_{L1} to Q_{L2} by increasing the rotor current to 1 p.u.

According to stator active/reactive power output and operating speed the rotor active power, reactive power, applied voltage and frequency must be varied so that the stator output voltage and frequency maintained constant at rated value. As mentioned before, DFIG can operates at two modes of operation when suppling a certain load. The first mode is sub-synchronous speed, DFIG rotational speed is chosen at 1350 rpm, where the DFIG rotational speed is less than the generator synchronous speed of 1500 rpm. The second mode is super-synchronous speed, DFIG rotational speed is chosen at 1650 rpm, where the DFIG rotational speed is greater than the generator synchronous speed.

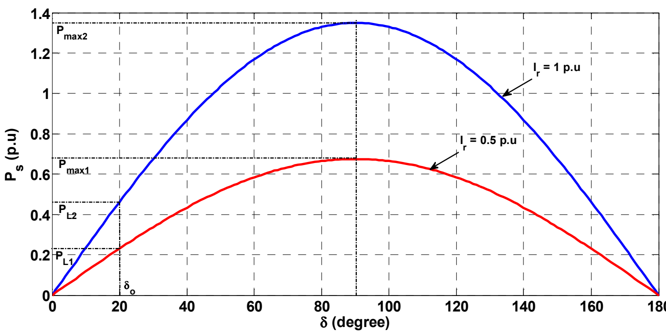

Fig. 5 Stator output active power, P_s, versus power angle δ at rotor current I_r = 1 and 0.5 p.u.

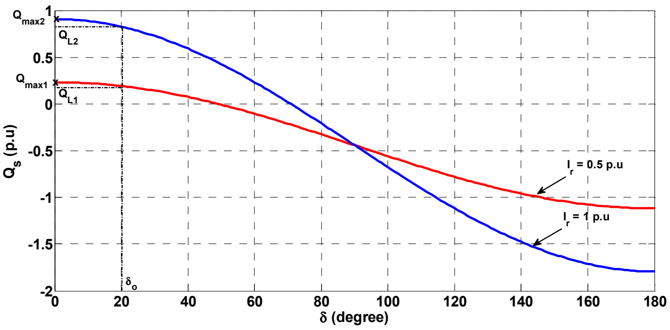

Fig. 6 Stator output reactive power, Q_s, versus power angle δ at rotor current $I_r = 1$ and 0.5 p.u.

Fig. 7 and Fig. 8 show the rotor active power, P_r, versus power angle δ at rotor current $I_r = 1$ and 0.5 p.u for sub- and super-synchronous speed modes of operation respectively. As shown, the P_r varies sinusoidally with δ. In sub-synchronous speed mode, the negative sign for P_r means the DFIG absorbs active power through the rotor terminals.

Also, in super-synchronous speed mode, the positive sign for P_r means the DFIG injects active power through the rotor terminals. For both two modes, increasing the rotor current, hence increasing the DFIG loading capability, leads to increasing the absorbed rotor active power from P_{r1_sub} to P_{r2_sub} in sub-synchronous mode and increasing the injected rotor active power from P_{r1_sup} to P_{r2_sup} in super-synchronous mode as the generator speed is held constant in each case.

Fig. 9 and Fig. 10 show the rotor reactive power, Q_r, versus power angle δ at rotor current $I_r = 1$ and 0.5 p.u for sub- and super-synchronous speed modes of operation respectively. The positive and negative sign for Q_r means the DFIG injects and absorbs reactive power through the rotor terminals in sub- and super-synchronous speed modes of operation. When the DFIG operates at sub-synchronous speed mode and stable region, the DFIG absorbs reactive power through the rotor terminals. While in case of super-synchronous speed mode and stable region, the DFIG injects reactive power through the rotor terminals. For both two modes, increasing the rotor current, hence increasing the DFIG loading capability, leads to increasing the absorbed rotor reactive power from Q_{r1_sub} to Q_{r2_sub} in sub-synchronous mode and increasing the injected rotor reactive power from Q_{r1_sup} to Q_{r2_sup} in super-synchronous mode as the generator speed is held constant in each case.

Fig. 11 and Fig. 12 show the magnitude of the rotor input voltage, V_r, versus power angle δ at rotor current $I_r = 1$ and 0.5 p.u for sub- and super-synchronous speed modes of operation respectively. As shown, the rotor voltage varies as the δ in order to maintain the rotor current at constant value for constant output voltage operation. Also, at stable region, Increasing the rotor current, hence increasing the DFIG loading capability, leads to increasing the required rotor voltage from V_{r1_sub} to V_{r2_sub} in sub-synchronous mode and from V_{r1_sup} to V_{r2_sup} in super-synchronous mode as the generator speed is held constant in each case.

B. Effect of speed variation on the DFIG operated at constant load

In this study, the DFIG is assumed to be operated at constant three different loads as follows:
Load 1 (L1): 21120 W.
Load 2 (L2): 15000 W and 14868 VAR.

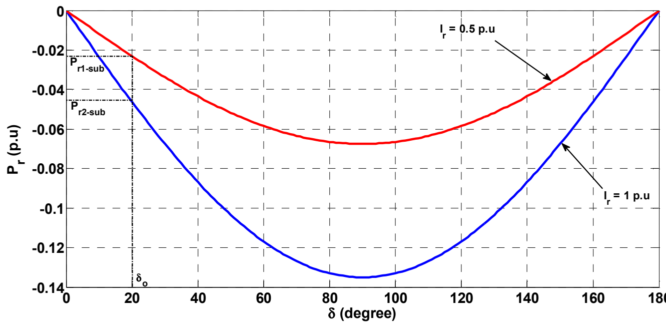

Fig. 7 Rotor active power, P_r, versus power angle δ at rotor current $I_r = 1$ and 0.5 p.u for sub-synchronous speed mode of operation.

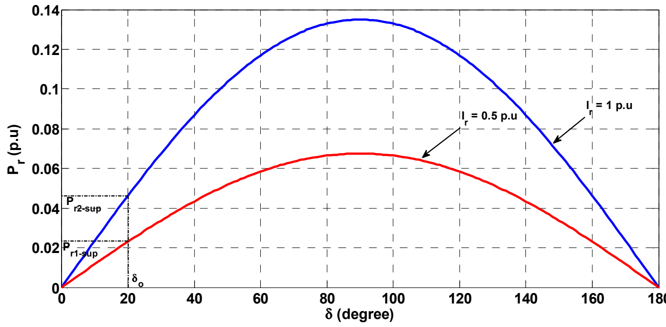

Fig. 8 Rotor active power, P_r, versus power angle δ at rotor current $I_r = 1$ and 0.5 p.u for super-synchronous speed mode of operation.

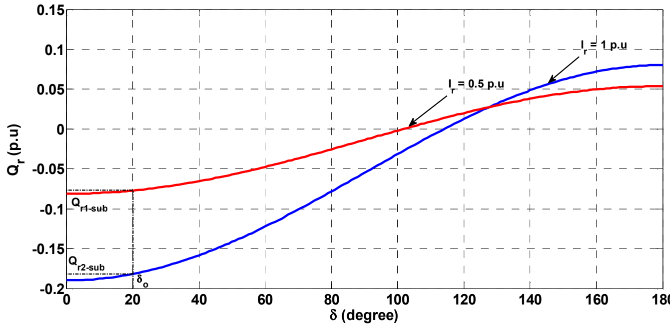

Fig. 9 Rotor reactive power, Q_r, versus power angle δ at rotor current $I_r = 1$ and 0.5 p.u for sub-synchronous speed mode of operation.

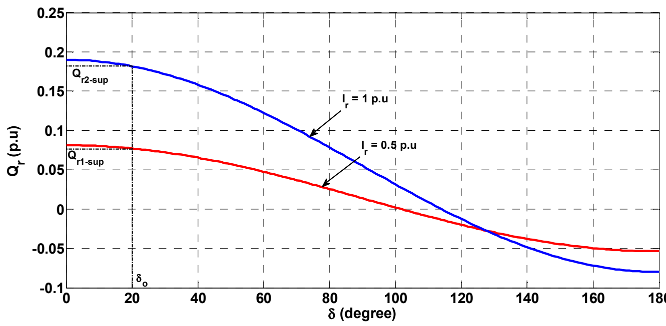

Fig. 10 Rotor reactive power, Q_r, versus power angle δ at rotor current $I_r = 1$ and 0.5 p.u for super-synchronous speed mode of operation.

Load 3 (L3): 14868 VAR.

While the DFIG operating speed is varied from 1050 to 1950 rpm during applying each load. Also, the DFIG is operated at constant output voltage and frequency for all operating conditions.

Fig. 13 shows the rotor active power, P_r, versus rotational speed, N, for different loading conditions of L1, L2 and L3. As shown for L1 and L2, at sub-synchronous speed mode, the higher the rotational speed the lower absorbed active power by the rotor.

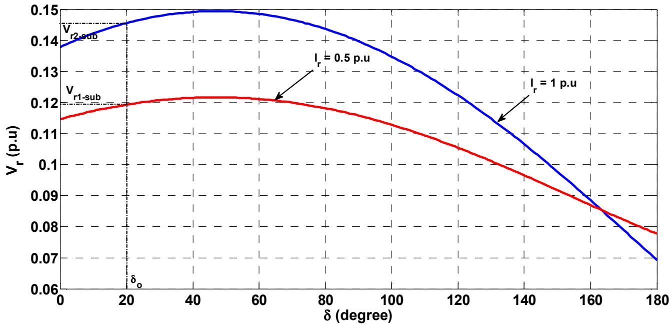

Fig. 11 Magnitude of the rotor input voltage, V_r, versus power angle δ at rotor current I_r = 1 and 0.5 p.u for sub-synchronous speed mode of operation.

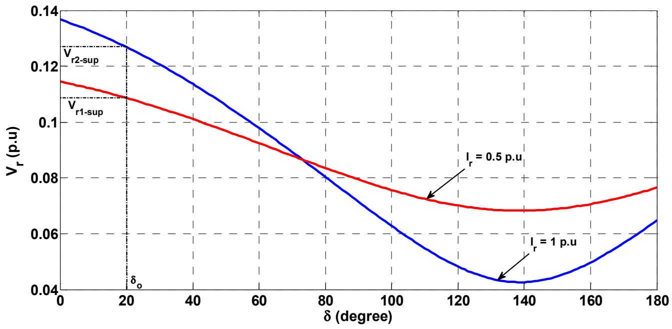

Fig. 12 Magnitude of the rotor input voltage, V_r, versus power angle δ at rotor current I_r = 1 and 0.5 p.u for super-synchronous speed mode of operation.

While for super-synchronous speed mode the higher the rotational speed the higher injected active power by the rotor.

Also, at certain rotational speed, as the load active power increases the active power absorbed or injected by the rotor increases. The rotor active power for L3 at all operating speed is zero as the load power is zero in this case.

Fig. 14 shows the rotor reactive power, Q_r, versus rotational speed, N, for different loading conditions of L1, L2 and L3. As shown for all loads, at sub-synchronous speed mode, the higher the rotational speed the lower absorbed reactive power by the rotor.

While for super-synchronous speed mode the higher the rotational speed the higher injected reactive power by the rotor. Also, at certain rotational speed, the reactive power absorbed or injected by the rotor depends on the load active and reactive power.

Fig. 15 shows the magnitude of the rotor input voltage, V_r, versus rotational speed, N, for different loading conditions of L1, L2 and L3. As shown for all loads, at sub-synchronous speed mode, the higher the rotational speed the lower required rotor input voltage.

While for super-synchronous speed mode the higher the rotational speed the higher required rotor input voltage. The minimum required rotor input voltage is accrued nearly around the synchronous speed.

V. Conclusions

In this paper the steady state analysis and characteristics of the stand-alone DFIG are presented in a similar way as the synchronous generator. The rotor of the DFIG is excited with a slip frequency voltages and currents via an RSC and a battery. A simplified mathematical model required for evaluation of the steady-state analysis and characteristics of the DFIG is developed.

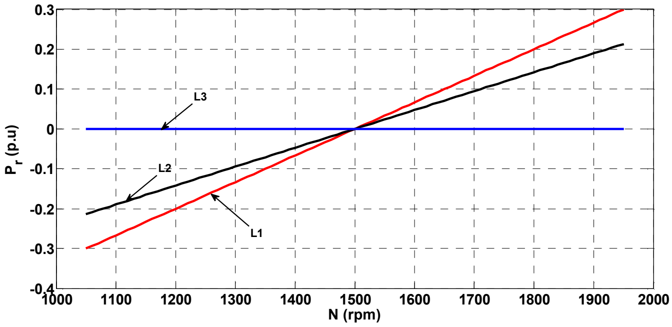

Fig. 13 Rotor active power, P_r, versus rotational speed, N, for different loading conditions of L1, L2 and L3.

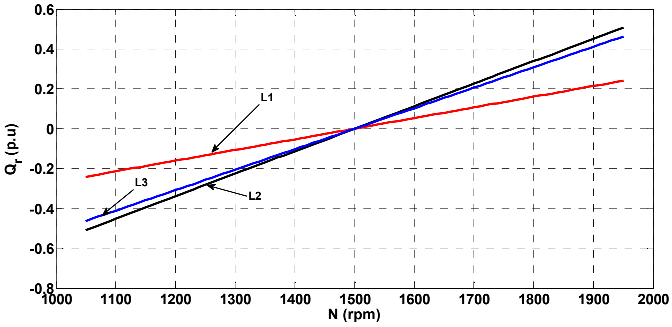

Fig. 14 Rotor reactive power, Q_r, versus rotational speed, N, for different loading conditions of L1, L2 and L3.

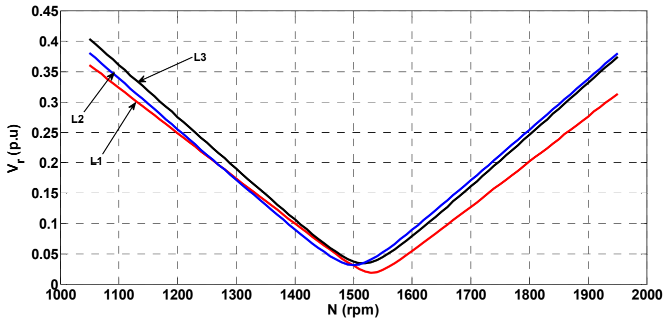

Fig. 15 Magnitude of the rotor input voltage, V_r, versus rotational speed, N, for different loading conditions of L1, L2 and L3.

The stator active and reactive power relations are expressed as a function of stator output voltage, rotor current, machine reactances, and the power angle. It is shown that the rotor active and reactive power relations are expressed in the same parameters as that for the stator active and reactive power relations with the rotor slip is taken into consideration.

The effect of changing the slip, rotor current, stator current, power angle, and load power factor on the magnitude of the required rotor voltage was presented. The presented work clearly illustrates the effect of the parameters of the DFIG on characteristics and performance of the generator when operated it at sub- and super-synchronous speed modes in stand-alone WECS application.

References

[1] L. Guo, D. Wang, Z. Peng and L. Diao, "Direct Voltage Regulation of A Stand-Alone DFIG System with Non-Linear Loads Based on An Improved-Extended State Observer and SSM control", *IET Renewable Power Generation*, vol. 13, no. 11, pp. 1891-1901, August 2019.

[2] S. Arnaltes, J.L. Rodriguez-Amenedo, M.E. Montilla-DJesus, "Control of Variable Speed Wind Turbines with Doubly Fed Asynchronous Generators for Stand-Alone Applications," *Energies*, vol. 11, no. 1, pp. 26, December 2017.

[3] R. D. Shukla, R. K. Tripathi, "Isolated Wind Power Supply System Using Double-Fed Induction Generator for Remote Areas," *Energy Conversion and Management*, vol. 96, pp. 473-489, 2015.

[4] I. Yasmine, E B. Chakib, B. Badre,"Improved Performance of DFIG-Generators for Wind Turbines Variable Speed", *International Journal of Power Electronics and Drive System (IJPEDS),* vol. 9, no. 4, pp. 1875-1890, December 2018.

[5] R. Arindya, "A Variable Speed Wind Generation System Based on Doubly Fed Induction Generator," *Bulletin of Electrical Engineering and Informatics*, vol. 2, no. 4, pp. 272-277, December 2013.

[6] R. D. Shukla, R. K. Tripathi, "A Novel Voltage and Frequency Controller for Stand-Alone DFIG Based Wind Energy Conversion System," *Renewable and Sustainable Energy Reviews*, vol. 37, pp. 69-89, 2014.

[7] F. Abdoune, D. Aouzellag, K. Ghedamsi, "Terminal Voltage Build-up and Control of a DFIG Based Stand-Alone Wind Energy Conversion System," *Renewable Energy*, vol. 97, pp. 468-480, 2016.

[8] R. Pena, J. C. Clare and G. M. Asher, "A doubly fed induction generator using back-to-back PWM converters supplying an isolated load from a variable speed wind turbine," *in IEE Proceedings - Electric Power Applications*, vol. 143, no. 5, pp. 380-387, September 1996.

[9] A. A. J. Jeman, N. M. S. Hannoon, N. Hidayat, M. M. H. Adam, I. Musirin, and V. Vijayakumar, "Stability check of doubly fed induction generator (DFIG) micro grid power system," *Bulletin of Electrical Engineering and Informatics*, vol. 8, no. 2, pp.367-374, June 2019.

[10] S. Soued, M. S. Chabani, M. Becherif, M. T. Benchouia, H. S. Ramadan, A. Betka, A. Golea, S. E. Zouzou, "Experimental Behaviour Analysis for Optimally Controlled Standalone DFIG System," *in IET Electric Power Applications*, vol. 13, no. 10, pp. 1462-1473, October 2019.

[11] N. K. Swami Naidu and B. Singh, "Experimental Implementation of Doubly Fed Induction Generator-Based Standalone Wind Energy Conversion System," *in IEEE Transactions on Industry Applications*, vol. 52, no. 4, pp. 3332-3339, July-August 2016.

[12] N. A. Elsonbaty, M. A. Enany and A. M. Diab, "Steady State Modelling and ANFIS Based Analysis of Doubly-Fed Induction Generator," *Michael Faraday IET International Summit 2015*, pp. 560-568, 2015.

[13] A. Alkandari, S. Soliman and M. Abdel-Rahman, "Steady State Analysis of a Doubly Fed Induction Generator," *Energy and Power Engineering*, Vol. 3 No. 4, pp. 393-400, 2011.

[14] R. Surya and S. Vadhera, "Novel Method for Steady State Analysis of Doubly-Fed Induction Generator Using MATLAB," *2016 IEEE 6th International Conference on Power Systems (ICPS)*, 4-6 March 2016, pp. 1-4.

[15] M. S. Vicatos and J. A. Tegopoulos, "Steady State Analysis of A Doubly-Fed Induction Generator Under Synchronous Operation," *in IEEE Transactions on Energy Conversion*, vol. 4, no. 3, pp. 495-501, September 1989.

[16] M. R. Islam, Y. Guo and J. G. Zhu, "Steady state characteristic simulation of DFIG for wind power system," *International Conference on Electrical & Computer Engineering (ICECE 2010)*, 18-20 December 2010, pp. 151-154.

[17] G. Ashwini Devendran, M. Jaikumar and P. Raja, "A simple methodology for the steady state analysis of Doubly Fed Induction Generator," *2012 Annual IEEE India Conference (INDICON)*, 7-9 December 2012, pp. 979-985.

[18] L. Makhlouf and S. Lassaad, "Steady state analysis of a doubly-fed induction generator," *2017 International Conference on Green Energy Conversion Systems (GECS)*, 23-25 March 2017, pp. 1-6.

[19] M. G. Simões and F. A. Farret, *Modeling and Analysis with Induction Generators*, Power electronics and applications series, third edition, Taylor and Francis Group, 2015.

[20] M. A. H. Salehy and M. N. Eskander, "Sub-Synchronous Range of Operation for A Wind Driven Double-Fed Induction Generator", *Journal of power Electronics*, vol.10, No. 1, January 2010.

[21] D. Santos-Martin, S. Arnaltes, and J. R. Amenedo, "Reactive Power Capability of Doubly Fed Asynchronous Generators," *Elect. Power Syst. Res.*, vol. 78, no. 11, pp. 1837–1840, 2008.

[22] M. Ahmed, M. EL-Shimy, M. Badr, "Advanced Modeling and Analysis of The Loading Capability Limits of Doubly-Fed Induction Generators," *Sustainable Energy Technologies and Assessments*, vol. 7, pp. 79-90, 2014.

[23] S. J Chapman, *Electric Machinery Fundamentals*, 5th ed., New York, McGraw-Hill, 2012.

[24] G. Abad, J. López, M. A. Rodrı´guez, L. Marroyo, G. Iwanski, *Doubly Fed Induction Machine Modeling and Control for Wind Energy Generation*, IEEE Press 445 Hoes Lane Piscataway, NJ 08854, November 2011.